2018 IEEE 15th International Conference on Mobile Ad-hoc and Sensor Systems

Sense and Deploy: Blockage-aware Deployment of Reliable 60 GHz mmWave WLANs

Zhicheng Yang*, Parth H. Pathak†, Jianli Pan‡, Mo Sha§, and Prasant Mohapatra*
*Department of Computer Science, University of California, Davis
†Department of Computer Science, George Mason University
‡Department of Mathematics and Computer Science, University of Missouri-St. Louis
§Department of Computer Science, SUNY Binghamton

***Abstract*—60 GHz millimeter-wave networks have emerged as a potential candidate for designing the next generation of multi-gigabit WLANs. Since the 60 GHz links suffer from frequent outages due to blockages caused by human mobility, deploying 60 GHz WLANs that can provide robust coverage in presence of blockages is a challenging problem. In this paper, we study blockage-aware coverage and deployment of 60 GHz WLANs. We first show that the reflection profile of an indoor environment can be sensed using a few measurements. A novel coverage metric (angular spread coverage) which captures the number of available paths and their spatial diversity is proposed. Additionally, it is shown that using relays can extend the coverage of the AP at a lower cost and provide added spatial diversity in the available paths. We propose a heuristic algorithm that determines the AP and relay locations while maximizing the angular spread coverage metric for the clients. Our testbed-based evaluation shows that for five different rooms, our proposed deployment can guarantee an average connectivity of 91.7%, 83.9%, and 74.1% of client locations in the presence of 1, 3 and 5 concurrent human blockages respectively, substantially increasing the robustness of 60 GHz links against blockages.**

I. Introduction

The emergence of millimeter wave (mmWave) networks has reinvigorated the quest of next generation of wireless networks that can provide multi-gigabit per second data rates. The 60 GHz millimeter wave band provides a large unlicense spectrum (57 - 64 GHz) where new wireless standards such as IEEE 802.11ad [1] and 802.11ay are proposed. The 802.11ad WLAN standard has shown to achieve per-link data rates of up to 7 Gbps, supporting applications like uncompressed video streaming, virtual and augmented reality. Due to their higher frequency, 60 GHz signals attenuate much faster compared to 2.4/5 GHz signals. This additional loss is compensated through the use of directional antenna where many antenna elements can be combined to form miniature phased antenna arrays that can fit in today's mobile devices. The phased antenna array provides the ability to electronically create and steer the beams in different directions to establish multi-gigabit links.

In this paper, we focus on coverage and deployment of access points in 60 GHz WLANs. mmWave signal propagation is substantially different in comparison to the 2.4/5 GHz spectrum used in legacy WiFi. First, 60 GHz mmWave signals attenuate significantly while penetrating walls and other indoor objects such as metal cabinets, wooden furniture, etc. This means that one 60 GHz AP is required in each room (or enclosed indoor space) to provide sufficient coverage. Second, blockage of a mmWave link from a human body results in a loss of 20 to 30 dB [2], essentially disconnecting the communication endpoints. Since human body blockage depends on human mobility patterns, the AP should be deployed in such a way that provides necessary backup paths (through reflections) for each client location. Both these requirements motivate us to design a novel deployment strategy for 60 GHz WLANs.

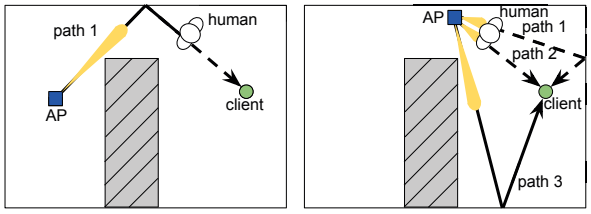

(a) Example of an AP placement where the client has only one path from the AP

(b) Example of an AP placement which has three spatially diverse paths between AP and client

Fig. 1: Two sample deployments of AP showing how AP location can give rise to more, spatially diverse set of paths to a client, increasing its tolerance to blockages

It is worth noting that AP placement in 60 GHz WLANs requires redefining coverage in terms of blockage. To further understand this, we provide an example in Fig. 1. It shows an indoor space with stationary blockages in the form of room layout and objects, and dynamic blockages in the form of a human. The AP placement shown in Fig. 1a covers the client through a reflected path from the AP. However, in the presence of a blockage, connectivity to the client is interrupted because there exists no other (first-order) reflection that can reach the client. Alternatively, if the AP was placed at a different location as shown in Fig. 1b, the existence of other reflected paths allows the AP to reach the client even in the presence of a blockage. *This way, the placement should not just cover a client, but it should do so with more number of paths and the paths should be spatially diverse. An ideal placement is the one where this condition is met for all clients for a given environment.* It is worth noting that the channel sparsity property of a 60 GHz channel restricts the number of dominant paths available to a few (on average 3-4 [3], [4]) in a typical indoor environment. Hence, the objective is to choose the AP location such that more and more number of client

2155-6814/18/$31.00 ©2018 IEEE
DOI 10.1109/MASS.2018.00063

locations have higher number of propagation paths to them and these paths are spatially diverse.

A. Challenges and Our Approaches

Deploying 60 GHz WLANs in a way that achieves high path spatial diversity for clients is difficult. We identify important challenges that need to be addressed and provide an overview of our solution below.

(1) Coverage metric for spatial diversity: Traditional coverage metrics (such as binary coverage where a client location is either covered or not) do not take into account the spatial diversity need of 60 GHz deployment. This means that there is a need of new coverage metric that quantifies the path diversity in a tractable way.

Contribution: We define a new coverage metric ASC (Angular Spread Coverage) based on the multi-path angular spread property of a millimeter-wave channel. For a given deployment of AP, ASC can quantify (1) the number of major paths available at a client location, (2) the spatial diversity of these paths and (3) the received power of the paths. Using the ASC metric, different AP deployments can be compared before choosing a suitable one.

(2) Sensing indoor reflection profile: In order to maximize the number of reflected paths available from the AP, the deployment should carefully consider the reflection profile of the room. However, it is challenging to accurately sense the indoor room layout and relative position of objects (blockages and reflectors). Relying on floor maps is undesirable due to their limited availability and their insufficiency in knowing the positions of objects/furniture insider the room layout.

Contribution: We propose to use a small set of pilot measurements to sense and construct the indoor layout which includes the relative positions of blocking and reflective objects. Instead of identifying the exact material of the objects, we rely on classifying them into either moderate or strong reflectors based on the measurements. We find that with our reflection loss estimation technique on an average 1 AP and 1 client per $10m^2$ of indoor space is sufficient for the pilot measurements and accurate reconstruction of room profile.

(3) Extension of coverage: Another important challenge in 60 GHz deployment is that all client locations in an enclosed indoor space might not be directly reachable through an AP. This is because even though the client locations might be within AP's communication range, due to the blockages presented by room objects/layout, the locations cannot be covered by the AP. Use of more APs can substantially increases the deployment cost.

Contribution: We present a solution where low-cost relays can be used to extend AP's coverage. The relays have been used recently in millimeter-wave cellular networks [5]. We propose to use relays with limited scanning range and different orientations that can directly connect to the AP and provide coverage to clients that are otherwise not reachable. The use of relays further complicates the deployment where the AP and relay placement should be jointly studied. Hence, we study the MACAR (MAximum Coverage using Single AP And Minimum Relays) problem which provides a joint solution for AP and relay placement in 60 GHz WLANs.

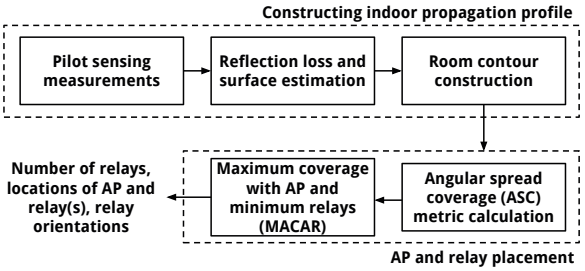

Fig. 2: System overview

(4) Complexity of 60 GHz AP/relay placement: Finding a solution to the above mentioned MACAR problem is computationally expensive due to many factors including a large number of possible locations (on the ceiling) for AP and relays, positions of different blockages and reflectors in a room, and many possible orientations of the relays.

Contribution: We show that the MACAR problem is NP-hard and provide a greedy strategy for AP and relay placement. The strategy aims at maximizing the summation of the ASC metric for all client locations using one AP and the minimum number of relays. We evaluate the strategy in five different types of rooms (different sizes and layout, for example, small living room, large office room, etc.) and find that using 2 relays on an average, MACAR can cover 88% of all possible client locations with at least two spatially diverse paths.

(5) Link reliability under multiple human blockages: Presence of multiple humans at arbitrary locations within an indoor space can substantially hamper the link reliability. Prior research [6], [3], [7] primarily considers single blockage but in reality, multiple blockages due to presence of more than one human being is likely in real-world. Our proposed deployment strategy should be able to tolerate multiple human blockages.

Contribution: We evaluate our system under the scenario of random multiple concurrent (human) blockages. We find that MACAR deployment can guarantee average connectivity of 91.7%, 83.9%, and 74.1% of clients in the presence of 1, 3 and 5 concurrent (human) blockages, respectively. Compared to a deployment that is agnostic of spatial diversity (captured through the ASC metric), MACAR deployment results in on an average 25%, 21.6% and 22.6% more connected clients for 1, 3 and 5 concurrent human blockages, respectively.

B. System overview

Fig. 2 provides an overview of our proposed approach for AP and relay placement for 60 GHz WLANs. First, a few pilot sensing measurements are collected in the room using two endpoints where one endpoint acts an AP and the other as a client. The measurements are collected for a pre-determined number of locations chosen for AP and client (a factor that we vary to understand its impact). We use our 60 GHz transmitter and receiver testbed to sense the surrounding objects and to collect Received Signal Strength (RSS) measurements. These sensing measurements are then used to estimate the reflection loss of different objects and classify them into strong or moderate

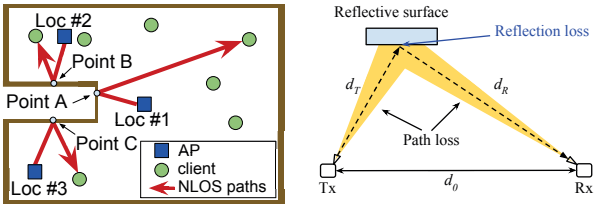

(a) Profiling a concave layout using multiple AP-client location pairs (b) Profiling four reflection points using a pair of AP-client

Fig. 3: Scanning measurements taken at pilot locations can be used to infer a room's layout and reflection profile

reflectors. This estimation of reflector type and its position derived from transmit and receive beamforming angles yield a discrete set of surface contour points. These points are then connected through a heuristic algorithm called genetic algorithm (approximation of traveling salesman problem) to construct the room contour.

The room contour represents the position of different blockages, the room layout, and the reflection type of different objects. This information is used by the AP and relay placement algorithm. Specifically, the contour is used for calculating the ASC metric for all client locations that need to be covered. The greedy strategy approximating the optimal solution to the MACAR problem uses the contour and coverage metric calculations to determine AP and relay locations. Our proposed strategy also determines the number of relays necessary and their orientations chosen to increase the client coverage.

The paper is organized as follows. Related work is discussed in Section V. The indoor propagation profile measurements and construction is discussed in Section II. The AP and relay placement strategy along with the coverage metric definition and calculations are provided in Section III. We evaluate the deployment techniques using our 60 GHz testbed in Section IV. We conclude in Section VI.

II. Sensing Indoor Room Profile

The room profiling involves the following steps: (1) Choose predetermined number of AP and client locations (referred as pilot locations here onward). For each pilot AP and client location combination, perform a complete 3-dimensional 360° degree scan with a pre-defined step angle. In the scanning, the two endpoints (AP and client) send and receive signals and record RSS for each transmit and receive angle. (2) For each transmit and receive angle and its observed RSS, estimate the reflection loss of the point. The reflection loss is then used to categorize the point of reflection (i.e. the object from which the signal reflected) in either a strong or a moderate reflector. (3) Lastly, generate the room contour through connecting the observed reflection points and estimated reflector type. We now discuss each step in more details.

A. Scanning using pilot locations

Ideally, a room can be profiled through the use of a large number of pilot AP and client locations, and performing exhaustive beam sweeping experiments to capture room's reflection profile. However, this kind of procedure will take a considerable amount of time and effort which is not practical. In our approach, we carefully select several pilot AP locations and randomly pick a limited number of pilot client locations in a given room. In order to obtain the reflection information, we rely on the scanning with 2° angular steps, and then leverage the Ray Tracing model [8]. Note that with electronic beamforming on phased antenna arrays, beam switching can be accomplished in nanoseconds which means that the complete scanning procedure can be completed in a short time. Given that majority of the large reflective/blocking objects (e.g., walls, metal cabinets, etc.) are likely to be moved much less frequently, the scanning procedure only needs to be performed once for each room.

Fig. 3a presents a room example with a concave shape in the layout. While the pilot AP is at the Location #1, the reflected point A can be obtained. However, without Locations #2 and #3, it seems difficult to obtain the reflected points B and C. In our experiments, we find that a corner pilot AP has a better capacity in profiling the blockages and reflections alongside the walls (e.g., the concave shape in Fig. 3a or other furniture against walls), while an AP location close to the center has better ability to profile ambient reflectors primarily due to higher signal incident angle which increases reflections. With more pilot AP and client locations, a better reflection profile can be yield albeit at a higher time and effort. However, we empirically evaluate that in 5 different types of rooms we study, on an average one pair of AP and client locations 10m^2 area is sufficient (i.e. yields very low contour estimation error) to profile an indoor space, Combined this with electronic beamforming, the scanning process can be completed efficiently without significant time and effort.

B. Reflection loss and type estimation

Once the measurements of transmit angle, receive angle and RSS are available through scanning, the next steps are (1) estimate the loss only due to reflection using the RSS and (2) use the reflection loss to categorize the object as either a moderate or a strong reflector.

Reflection Loss Estimation: Fig. 3b shows an illustration with reflection loss. The transmitted signal traverses distance d_T before striking the object's reflective surface. The reflected signal then traverses distance d_R before reaching the receiver. The permittivity of the object indicates how much of the signal that penetrates the object and reflects from it. Aside from the penetration and reflection, the signal is also absorbed by the objects and scattered from its surface. However, the absorption and scattering effect are difficult to measure in our system. Instead, we leverage the reflection loss due to the different permittivity as the approach to estimate the reflector type of the surface. If the transmission power is P_T, the transmit antenna gain is G_T, the received power is P_R, and the receiver antenna gain is G_R, the total loss $L = (P_T + G_T + G_R) - P_R$ is used to calculate the reflection loss as $L = L_P(d_T) + L_P(d_R) + L_R(\epsilon_o)$, where $L_R(\epsilon_o)$ is reflection loss from the surface with permittivity of ϵ_o, d_T and d_R are the distances of the object from the Tx

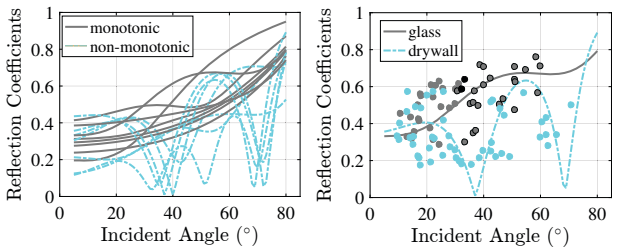

Fig. 4: (left) Reflection coefficients of various indoor materials (one line represents one material); (right) Using k-means clustering to categorize the reflection points in strong or moderate reflectors

and Rx respectively. The path loss $L_P(d)$ at distance d can be calculated using Friis model of free-space attenuation as $L_P(d) = 20\log_{10}(4\pi d/\lambda)$, where λ is the signal wavelength. The pilot AP and the pilot client have the knowledge of P_T and P_R, and the distance between them (d_0). As shown in Fig. 3b, d_T and d_R can be calculated using the transmitting angle and the receiving angle to derive $L_P(d_T)$ and $L_P(d_R)$. Using the equations above, the reflection loss $L_R(\epsilon_o)$ can be calculated, which will be used to estimate the reflector type of point in the next step.

Reflector Type Estimation: Once the reflection loss is estimated for the points, we are now interested in estimating the reflector type of the point (i.e., the object). This is challenging because various indoor reflective materials, such as walls, glass windows, whiteboards, etc., have different permittivities at 60 GHz, resulting in different reflection behavior. The reflection coefficient is a metric to measure the reflectivity of a material, which can be calculated from the permittivity as:

$$\Gamma = \frac{1-\exp(-j2\omega)}{1-\Gamma'^2\exp(-j2\omega)}\Gamma', \quad \Gamma' = \Gamma_\perp \text{or } \Gamma_\parallel \qquad (1)$$

where $\omega = \frac{2\pi D}{\lambda}\sqrt{\epsilon_2/\epsilon_1 - \sin^2\gamma}$, D denotes the thickness of the reflecting surface, λ is the signal wavelength, γ denotes the incident angle, ϵ_1 and ϵ_2 are the permittivities of the first medium and the second medium, respectively. In a single layer model, the first medium ϵ_1 can be assumed as air with the permittivity of 1. $\Gamma_\perp$ and $\Gamma_\parallel$ are the Fresnel's reflection coefficients when the electric field is perpendicular and parallel to the incidence plane, respectively.

We calculate the reflection coefficients of different room materials typically used using their permittivities [9], [10]. Fig. 4a shows the reflection coefficients for different incident angles. We observe that there are two set of curves - monotonic and non-monotonic. The monotonic curves refer to materials such as metal, glass, concrete, etc. while the non-monotonic curves refer to wooden objects. The metal and glass objects typically exhibit higher density and smoother and flatter surface compared to the wooden objects which results in different trends of reflection coefficient with varying incident angles. We leverage this information to classify the reflection loss of observed points into two categories - metal-like strong reflectors and wooden-like moderate reflectors.

The database developed in Fig. 4a is used for classifying the measured reflection points into strong or moderate reflector based on their reflection loss. As shown in Fig. 4b, the measured reflection points are scattered based on their incident angle and reflection loss. K-means clustering algorithm is then applied to these points to match them against the Fig. 4a curves. Here, K is chosen to be 2 since we are only interested in categorizing the points to be strong or moderate reflectors. Fig. 4b shows that in a sample room, the points match two pre-calculated curves for glass and drywall. Note that we are not interested in uniquely identifying the object material (i.e., glass, wood, metal, etc.). This is because identifying the object requires precise estimation of reflection loss along with the scattering and penetration loss. Our system is incapable of measuring the scattering loss. Using this procedure, we are able to assign a reflector type to each of the measured reflection point.

C. Room Contour Construction

Each of the points and its estimated reflector type are now connected to generate the contour of the room. We model the contour generation problem as the Traveling Salesman Problem (TSP). Given the TSP problem is NP-hard, we use a well-known approximation heuristic algorithm called genetic algorithm for contour generation. The surfaces such as glass windows, fridge's metal surface are categorized as strong reflectors while drywalls and wooded door surfaces are categorized as moderate reflectors. Note that once all reflected points are connected to construct a contour, it is converted to an isothetic shape. The error in room contour construction compared to the ground truth room layout is captured through Hu Moment Invariants (HMI) [11]. The HMI is a well-known method in computer vision to describe a contour consisting of the shape and location of segments/blocks. One of its criteria quantifies how well two contours match using geometric distances. We refer to this criterion as the HMI score and use it in our purpose to reflect the error (mismatch) in contour matching. As we show in the evaluation, the reflection loss and type estimation, and genetic algorithm can accurately construct the room contour (low HMI score).

III. Relay-assisted AP Placement

Based on the room contour constructed in Sec. II, we now provide the details of our AP and relay placement strategies. Since the placement strategies are dependent on the definition of coverage, we first introduce the coverage metrics specific to our objectives.

A. Angular Spread Coverage

Traditionally, a coverage metric refers to a binary value representing whether a client location is covered by the AP or not. We refer to this metric as "Binary Coverage" (BC). Each covered location under this concept has necessary RSS from AP to support the smallest Modulation and Coding Scheme (MCS) (For example, in 802.11ad, MCS 0 requires at least -78 dBm SNR [1]) over at least one (either LOS or reflected) path. The objective of AP placement for this BC metric is to maximize the number of covered client locations by the AP.

AP placement based on the BC metric aims at covering a set of client locations, however, it does not guarantee any robustness in the resultant connectivity. As we discussed using Fig. 1a in Section I, we are interested in designing a deployment strategy that not only covers clients but it does so with more number of paths and these paths are spatially diverse. Such a deployment will be more robust to blockages given that there are more number of backup paths available between clients and the AP.

Angular spread based coverage metrics: The spatial diversity aforementioned can be captured and quantified using the *angular spread* originally proposed in [12]. Consider an angular distribution of incoming power $p^{AS}(\theta)$ for a given client location. The discrete set of paths available in an angular power distribution is often referred as *path skeleton* which is a sparse set of dominating paths which approximately represent the spatial channel of a 60 GHz link [3] of a millimeter-wave channel. If the client has one LOS path and one reflected path from the AP, then $p^{AS}(\theta)$ will be largely concentrated in two direction between 0 and 2π. Now, let F_q be the q_{th} Fourier transform of $p^{AS}(\theta)$ as

$$F_q = \int_0^{2\pi} p^{AS}(\theta) \exp(jq\theta) d\theta. \tag{2}$$

The angular spread Λ^{AS} is defined as

$$\Lambda^{AS} = \sqrt{1 - \frac{|F_1|^2}{|F_0|^2}} \tag{3}$$

If the channel model is the two-wave channel model, $p^{AS}(\theta)$ is defined as $p^{AS}(\theta) = P_1\delta(\theta - \alpha) + P_2\delta(\theta - \beta)$, where P_1 and P_2 are the power of signals arriving from the corresponding angles in the azimuth plane, and α and β are the angles of arrival. Although angular spread can represent the spatial diversity of a client's signal paths, it is not readily useful for our purpose. This is because the angular spread in its original normalized form (1) is unable to distinguish the number of paths if their interval angles are equal; (2) has the value of zero in one-path channel , which fails to capture that the client is still connected. Therefore, we derive a generalized form of the angular spread to distinguish the skeleton's angular symmetry with the awareness of one-way channel model.

$$\Lambda = \frac{P' + \sqrt{|F_0|^2 - |F_1|^2}}{P''} \tag{4}$$

where

$$F_q = \int_0^{2\pi} p(\theta) \exp(jq\theta) d\theta \tag{5}$$

$$p(\theta) = P_1\delta(\theta - \alpha) + P_2\delta(\theta - \beta) + ... \tag{6}$$

where $\{\alpha,\ \beta,\ ...\}$ are the angles of arrival of a skeleton, and $\{P_1,\ P_2,\ ...\}$ are the individual powers arrive at the corresponding angle at the azimuth plane. Based on this generalized form, we derive a new metric, called Angular Spread Coverage (ASC). In ASC, P' and P'' are set as P_{max}, which is the maximum power of $\{P_1,\ P_2,\ ...\}$. We denote Λ in ASC as Λ^{ASC}. For any given AP location, ASC metric for client locations can be calculated using room contour which includes the location and type of reflectors within the room.

B. AP and Relay Placement

Using the ASC metric, we now turn our focus on the AP and relay placement. We first discuss how utilizing a relay can improve the coverage at a lower cost.

Limitation of a single AP: In an empty indoor space, all client locations are covered by the AP using an LOS path as long as the path provides RSS necessary for the minimum MCS (MCS 0 in 802.11ad). However, the room layout and objects can introduce blockages to make certain parts of the indoor space unreachable directly from the AP. To deal with the actual scenarios of this kind, it is possible to deploy additional APs. However, this increases the deployment cost substantially as each new AP requires a wired connection. Wireless relays have been proposed to overcome this cost issue. Specifically in millimeter-wave, the relays have been used in cellular networks and in indoor environments recently [5], [13]. Compared to AP, relays are simpler in design and provide a cheaper solution for coverage extension. Therefore, we leverage relays to extend the connectivity of an AP.

Heterogeneous system of AP and relays: Even though the relays are cheaper and effective solution for providing a better coverage, one challenge is that they have to be directly connected (over an LOS path) to the AP for relaying the data. A mmWave relay proposed in [13] uses phased array antennas to perform beamforming. Such a relay's coverage range, the maximum distance a relay can reach, is limited towards its facing direction and scanning angle. We assume that the AP does not suffer from beam distortion as it is equipped with multiple phased antenna patches if necessary. However, a relay's coverage range, the maximum distance a relay can reach, is limited towards its facing direction and scanning angle. Such a comprehensive AP and relay system is still a *heterogeneous* because of differences in AP's and relay's coverage range and scanning angle. For simplicity, we assume that all relays are homogeneous which means that they have the same coverage range and a finite set of facing directions, which are referred as *orientations*.

MAximum Coverage using Single AP And Minimum Relays (MACAR): Our objective is to deploy AP and relays at carefully chosen locations so that the maximum number of clients are covered by one AP and the minimum number of relays. Given one of the two metrics (BC or ASC) as the choice of coverage metric, the aim is to find location of the AP and relays that results in maximum summation of the metric for each covered client using the minimum number of relays. Note that placing an AP at any given location results in a specific value of the metric for each client location. More number of clients are covered by adding the relay which can also increase the metric score of clients already covered by the AP.

We denote the number of clients that need to be covered as l, and the number of homogeneous relays can be used as m. A single AP has the coverage range r_A, while each relay has n orientations, the coverage range r_R, and the scanning angle Δ. Given a set of clients $\mathbb{C}$, an AP can cover a subset of $\mathbb{C}$, while each relay is supposed to switch its discrete orientations

to cover different subsets of $\mathbb{C}$. Therefore, two sets $\mathbb{A} = \{A_a\}$ and $\mathbb{R} = \{R_b^c\}$ can be achieved, where A_a is a subset of $\mathbb{C}$ when the AP is at the location of the relay a, and R_b^c is a subset of $\mathbb{C}$ using relay b and orientation c, $1 \leq a \leq m$, $1 \leq b \leq m$, $1 \leq c \leq n$. The problem is to find a set $\mathbb{D}$, consisting of $\{A_a, \mathbb{R}'\}$, where $\mathbb{R}' \subseteq \mathbb{R}$. Every selected relay R_b^c in $\mathbb{R}'$ must communicate to the AP within its coverage range and scanning angle, and consists of at most one $\{R_b^c\}$ for each b. It means that only one orientation c can be activated for each resultant relay b. The objective is to maximize the summation of one chosen coverage metric of each element in $A_a \bigcup R_B^C$ and minimize $|\mathbb{R}'|$, where R_B^C is the union of R_b^c in $\mathbb{R}'$ for every selected b and c, and the intersection of a and B is zero since the relay cannot overlap the AP location.

Complexity of MACAR: We show that MACAR is an NP-hard problem. According to the definition of NP-hard problems, one problem is NP-hard if it can be reducible to an existing NP-hard problem in polynomial time (i.e., at least as hard as an existing NP-hard problem). The MACAR problem is similar to a well-studied problem in wireless sensor networks called Effective Coverage Problem (ECP) where the objective is to provide sensing coverage to a given area/points using the minimum number of sensors (assuming each sensor has a sensing and communication range). Authors in [14] showed that the ECP can be formulated as the minimum cost set covering problem, which is a well-known NP-hard problem [15]. It means that ECP is reducible to the set cover problem, so ECP is an NP-hard problem as well.

We now show that MACAR is reducible to ECP. Although ECP focused on omni-directional sensor networks, the omni-directional propagation can be divided by multiple sectors. We are then able to transform the omni-directional sensor network problem to our directional relay problem. Following this conception, we denote R_1, R_2, ..., R_m for m sensors as their respective subset of covered targets in ECP, and then duplicate each of them with n orientations and denote them again as R_1^1, R_1^2, ..., R_1^n, R_2^1, ..., R_m^n. This way, the MACAR problem is an generalized version of ECP, and can be reduced to ECP in a polynomial time. Note that ECP has pre-defined sensing range and communication range of every sensor. Those parameters are independent with the complexity of ECP. Similarly in MACAR, the coverage range and scanning angle of AP and each relay is pre-defined, and those are also independent with the procedure of MACAR. Hence, the MACAR problem is also an NP-hard problem.

Greedy Algorithm for MACAR Given that the MACAR problem is NP-hard, we propose a greedy algorithm to approximate the MACAR solution. Greedy algorithm is a widely used as an approximation algorithm in many recent deployment problems [16], [14]. Algorithm 1 shows our proposed greedy strategy to yield an approximate solution for the NP-hard MACAR problem. The algorithm takes as input the chosen metric (BC or ASC), set of clients to be covered and set of candidate locations for AP and relay(s). It first selects an AP location from the candidate locations such that the sum of the metric is maximum for the clients it covers through that location. Once the AP location is determined, more relays are iteratively added to cover more client locations. For each newly added relay, it is ensured that the relay is directly able to communicate with the AP and its orientation is also chosen accordingly. The procedure stops when adding more relays no longer increases the number of covered clients. The limitation primarily stems for the fact that the relay should be connected to the AP in one hop. Algorithm 1 outputs the AP location and location(s) and orientation(s) for the relay(s). In the worst case, the algorithm will turn only one client as covered in each loop of sensor traversing, so it will take total m loops at the most. In such a case, the algorithm will make mnl comparisons for the number of relays, orientations and clients. Hence, the complexity of MACAR is $O(m^2nl)$.

Algorithm 1 Greedy Algorithm for MACAR

Input:
Coverage metric Λ (Λ^{BC} or Λ^{ASC});
Set of uncovered clients;
AP and relay location candidates

Output:
AP location; location(s) and orientation(s) of relay(s)

Procedure:
1: Choose the AP location in such a way that $\sum \Lambda$ for clients it covers is the maximum
2: For the AP location chosen, select a subset of candidate relay locations and their orientations that can directly communicate with the AP
3: Remove the clients covered by the AP from the set of uncovered clients
4: **while** 1 **do**
5: Choose a relay location and its orientation such that $\sum \Lambda$ for clients it covers is the maximum
6: **if** no new clients can be covered by adding the relay (with any orientation) **then**
7: BREAK;
8: **else**
9: Remove the clients covered by the relay from the set of uncovered clients
10: **end if**
11: **end while**

IV. Evaluation

A. Experiment Setup

Due to the unavailability of reconfigurable off-the-shelf 60 GHz transmitter and receiver devices, we build our testbed (AP and client) using WARPv3 [17] software radio and high-speed ADC/DAC as the baseband signal generator and processor. The WARP radio is connected to VubIQ 60 GHz development board [18] which provides the millimeter-wave RF front-end. Fig. 5a shows the AP side which includes a high-precision motorized rotator and tripod imitating a ceiling mounted AP. Due to the unavailability of reconfigurable phased antenna array for electronic beamforming, we rely on a horn antenna with the 3-dB beamwidth of 12° [18] connected with a waveguide which in turn are mounted on the rotator for

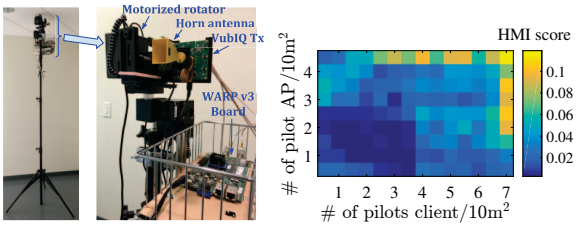

(a) (b)

Fig. 5: (a) 60 GHz transmitter setup to imitate a ceiling mounted AP; (b) HMI score with different pilot AP and client densities

mechanical beamforming. The client configuration uses the same setup except the tripod is set at a different height.

We evaluate the AP placement in five different type of rooms: (1) Conference room (area: 21.67 m^2), (2) Office room (area: 43.48 m^2), (3) University lab room (area: 67.01 m^2), (4) home living room (area: 44.68 m^2), and (5) home bedroom (area: 23.68 m^2). These rooms are chosen to cover a diverse set of possible indoor settings (different layouts, furniture, indoor materials, etc.). For each of the rooms, we set the height of the pilot AP to be 2.5m to imitate ceiling mounted AP. The height of the client is set to 1.2m to emulate mobile devices carried by users in their hands or lying on the desks.

We set the horizontal distance of 0.3m as the reference 0 dB RSS loss, and determine the AP's coverage range to be the largest distance corresponding to 25 dB, which is the loss between the RSS value corresponding to the maximum data rate of single carrier MCS and the RSS value corresponding to the minimum control rate MCS. We set the relay gain to be 10 dBi as in other relay-assisted systems [19].

B. Indoor profiling and contour construction

As discussed in Sec. II, the accuracy with which we can construct the room contour and identify reflective objects depends on the characteristics of the pilot measurements. One major factor that affects the accuracy is the number of pilot APs and client locations chosen while performing the reflection measurements. We use the HMI score (described in Section II) to evaluate the accuracy of our contour construction (similarity between the actual room layout and the estimated contour). Using the pilot AP and pilot client setup described before, we perform extensive measurements in the above mentioned five rooms. For each room, we vary the number of pilot AP locations from 1 to 9 and pilot client locations from 1 to 15, resulting in a set of 135 measurements per room. The pilot AP and client locations are uniform randomly chosen within the room following the grid anchor points for reference. The grid resolution is set as 0.6 meter. We then use each of the 135×5 measurements to construct a contour. Fig. 5b shows how the accuracy of contour construction (HMI score) varies with different number of pilot APs and clients. Due to the difference in area of each room, we represent the number of APs and clients in the form of density i.e. the number of APs or clients per $10m^2$.

As we can observe from Fig. 5b, the lowest HMI score is achieved when the number of pilot clients per $10m^2$ is $1 \sim 3.5$ and the number of pilot APs is $1 \sim 2.5$ per $10m^2$. In fact,

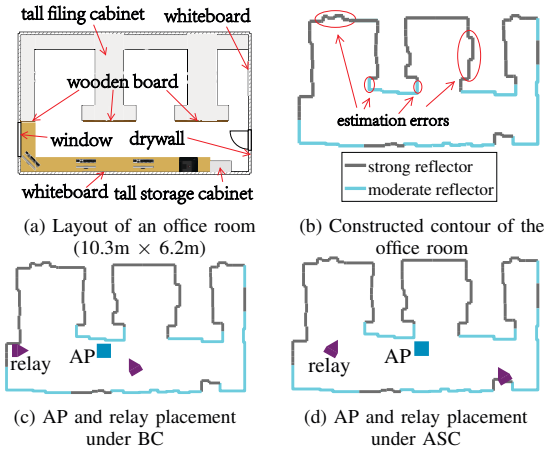

(a) Layout of an office room (10.3m × 6.2m)

(b) Constructed contour of the office room

(c) AP and relay placement under BC

(d) AP and relay placement under ASC

Fig. 6: ASC and BC based deployments result in different placement of AP and relays because ASC aims at covering clients with more spatially diverse paths

on an average 1 AP and 1 client per $10m^2$ in indoor space area is sufficient to achieve a very low HMI score (less than 0.02). It is interesting to observe that increasing the number of pilot AP and client locations does not necessarily result in better contour estimation. This is because more number of reflection points leads to increasing mismatch in clustering based on the reflection loss. Also, more points results in fine-grained share construction which in combination with errors in reflection loss estimation results in sawtooth shapes and denticles in contour generation using the genetic algorithm. Because of our current setup is limited to measuring coarse-grained RSS and not detailed channel state (such as signal phase), increasing the pilot locations results in higher error.

Note that even though an appropriate number of pilot APs and pilot clients is used, the constructed contour still has non-zero estimation errors. Fig. 6a and 6b show the actual plan and estimated contour of an office room. The errors are due to the process of converting the connected contour from the genetic algorithm to an isothetic shape. In this conversion, additional broken-line surfaces will be created which are not assigned with some reflective surface type. Those surfaces have to be determined by the existing surface type of adjacent reflected points. However, even though with some estimation errors, the constructed contour has been able to match most of shape and surface locations.

C. AP Placement Estimation

Number of relays: We now evaluate the performance of our greedy algorithm for AP and relay placement. The contour estimated for the five rooms are used as input to the placement algorithm. We assume that every grid point in the room is a potential client location which means that the algorithm will try to cover as many points as possible within the room. Since the conference room has the simplest layout, it is observed that the AP placement decision for both BC and ASC metric is identical for the room. Fig. 8a shows that due to minimal obstructions in the conference room, all clients locations are directly connected through the AP. This eliminates the need of having any relays deployed in the environment. The results

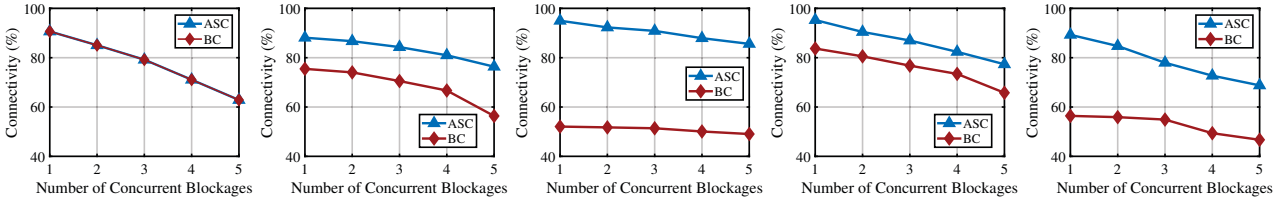

(a) Conference room (b) Office room (c) Lab room (d) Home living room (e) Home master bedroom

Fig. 7: Percentage of connected clients (% connectivity) under the two metrics in five rooms with concurrent blockages; As number of concurrent blockages increase, ASC-based deployment provide substantially better tolerance to blockages

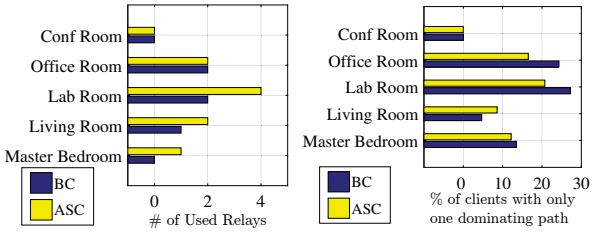

(a) Number of relays used in the placement under two metrics (b) Percentage of clients with only one dominating path to AP

Fig. 8: MACAR deployment reduces the number of client locations that are covered with fewer paths

show that in the rooms where there are minimal number of obstructions, AP can be placed at the center of the ceiling as it achieves the maximum path diversity for all client locations.

Considering more complex indoor layouts, Fig. 6a shows the layout of the office room considered in the study. As shown in Figs. 6c and 6d, the BC and ASC metrics result in use of two relays through the greedy algorithm. The locations of the AP and relays are substantially different because the ASC metric tries to cover clients with spatially diverse paths. Note that in both ASC and BC deployments shown in Figs. 6c and Fig. 6d, no additional relay can be added such that it covers more clients and is still connected to the AP. To further understand the performance of AP and relay placement, Fig. 8a shows the number of relays used with BC and ASC metric in the five rooms. We find that when room contour is more complex (for example, concave layouts) and area is larger, more number of relays are used in the room. It is also observed that use of ASC metric results in more number of relays compared to the BC metric. This is expected given that the ASC metric tries to more aggressively cover the clients using more number of spatially diverse paths.

Tolerance to blockage: Fig. 8b shows the percentage of clients that are connected with only one dominant propagation path after the AP and relay deployment. The purpose of studying this is that these clients will be highly vulnerable to any blockages which can disconnect their only path to the AP or relay. Since BC metric primarily focuses on increasing the number of clients covered, it results in a higher percentage of clients with one path. On the other hand, ASC results in fewer such clients in almost all layouts as the metric is designed to capture the number of paths and spatial diversity of the paths. Recent studies [3] shows that when a transmitter and a receiver are deployed at randomly chosen location in different indoor environments, the endpoints have only one dominant propagation path in on average 40% of instances. We show that when the AP is carefully deployed using ASC metric, the percentage of one-path clients reduce to 11.6% (average across the clients in five rooms). This further substantiates our claim that environment characteristics can be exploited in order to increase the tolerance to blockages.

To further evaluate the tolerance to blockages in the resultant AP/relay placement, we introduce blockages at randomly chosen locations which affect arbitrary number of clients. This emulates a real-world scenario where random blockages are introduced by human mobility. The blockage size is chosen to be a square of $0.3m \times 0.3m$ to match the size of a typical human. Furthermore, we increase the number of *concurrent blockages* to study the impact of multiple people walking in a room when AP/relays are deployed using the ASC metric. Fig. 7 shows the average percentage clients connected for the deployments in five rooms using the two metrics as the number of concurrent blockages increases. We observe that BC-based deployment suffers from significantly more percentage of clients disconnected as it does not deploy the AP and relays to increase the number of spatially diverse paths. On the other hand, the percentage of clients connected decreases slowly in comparison for the ASC-based deployment because it guarantees more number of spatially diverse paths for the clients. ASC-based deployment results in on average 25%, 21.6% and 22.6% more connected clients compared to BC-based deployments when the number of concurrent blockages are 1, 3 and 5 respectively.

We observe that the chosen AP location plays an important role along with number of relays in providing blockage tolerance. Since the placement of the AP and the number of relays used for both metrics are identical for the conference room, their percentage connected clients also vary similarly with varying number of blockages (Fig. 7a). On the other hand, the AP location chosen by the greedy algorithm using ASC metric is very different from the one chosen for BC metric in the lab room. This along with more number of relays used in the lab room (Fig. 7c) significantly changes the percentage of connected clients in the presence of blockages. For the living room scenario, the percentage of one-path clients are actually more in ASC-based deployment (Fig. 8b), however, the percentage clients that remain connected after blockage are fewer for the BC-based deployment (Fig. 7d). This is due to the fact that BC-based deployment results in high number of clients with two propagation paths which reduces its tolerance especially in case of concurrent blockages.

V. Related Work

60 GHz propagation characterization: Exploration of propagation characteristics of 60 GHz millimeter wave signal had started over a decade ago. As part of the early research, authors in [4] measured the power delay and angle profiles of 60 GHz channels in an indoor environment. To better understand indoor reflections, [20] measured the reflection characteristics of a variety of building materials (e.g. wall, partitions etc.) of different thickness and roughness, and derived reflection coefficients. Recently, Authors in [2] measured the capacity and coverage of a 60 GHz link in indoor environment with comprehensive investigation of reflection from indoor objects/materials and impact of human blockage. The primary focus of the previous studies have mostly been point-to-point links, while our research will also focus on the design and deployment of 60 GHz WLANs. Our research is also in agreement with the initial feasibility study of 60 GHz WLANs presented in [21] and focuses on the problem of coverage and deployment of 60 GHz WLANs.

60 GHz WLANs and reliability: Beam switching and beamwidth dilation have been studied as two main solutions for dealing with blockage and mobility. Authors in [6] use probe frames to check if the current path is blocked before sending the actual data frame. If the path is blocked, beam switching or dilation is employed. In a different approach, [3] showed that blockage of one beam affects the performance of other beams, and their correlation can be used to switch the beam without any probing. Authors in [22] relied on the client device motion sensors to determine its heading direction and speed. Using a multi-level codebook, the beam is switched or dilated based on the mobility and blockage. These techniques of beam switching benefit from our AP/relay placement research because proper deployment enables more spatially diverse paths that can be leveraged by intelligent beam switching techniques. Recently, [7] has proposed a similar approach for sensing ambient reflectors and using the inferences for deployment. However, our work addresses two critical outstanding issues. First, we propose and formalize a novel coverage metric which is essential to quantify the reliability of coverage provided by a deployment. Due to this, after sensing the indoor profile, our deployment strategy can provide guaranteed coverage in presence of one or more human blockages. Second, different from [7], our deployment strategy includes determining the number of relays, their location and orientation, to provide the coverage guarantee.

VI. Conclusions

In this paper, we presented a 60 GHz access point and relay placement approach which aims at increasing the number of available paths and their spatial diversity at the clients. We presented a metric based on angular spread that can capture the path diversity and drive the AP and relay deployment. A measurement-drive contour construction technique was outlined which essentially locates the strong and moderate reflectors. This information is then used by the placement algorithms to improve the path diversity metric for the clients. Our tesbed-based evaluation in five rooms show that the proposed deployment can substantially increase the client connectivity compared to the binary coverage metric where 91.7%, 83.9%, and 74.1% of clients remain connected in the presence of 1, 3 and 5 concurrent (human) blockages respectively.

Acknowledgement

We would like to thank Dr. Qingyun Wang from University of Oregon, Fanyi Xiao, and Dr. Yong Jae Lee from UC Davis for their comments and suggestions. This research is supported by the NSF through grant CNS-1730083 and grant CRII-1657275 (NeTS).

References

[1] IEEE P802.11adTM/D4.0, "Wireless LAN MAC/PHY Spec.: Enhancements for Very High Throughput in the 60 GHz Band," 2012.

[2] S. Sur, V. Venkateswaran, X. Zhang, and P. Ramanathan, "60 ghz indoor networking through flexible beams: a link-level profiling," in *ACM SIGMETRICS*. ACM, 2015.

[3] S. Sur, X. Zhang, P. Ramanathan, and R. Chandra, "Beamspy: enabling robust 60 ghz links under blockage," in *USENIX NSDI 16)*, 2016.

[4] H. Xu, V. Kukshya, and T. S. Rappaport, "Spatial and temporal characteristics of 60-ghz indoor channels," *IEEE Journal on selected areas in communications*, vol. 20, no. 3, pp. 620–630, 2002.

[5] S. Biswas, S. Vuppala, J. Xue, and T. Ratnarajah, "On the performance of relay aided millimeter wave networks," *IEEE Journal of Selected Topics in Signal Processing*, vol. 10, no. 3, pp. 576–588, 2016.

[6] M. K. Haider and E. W. Knightly, "Mobility resilience and overhead constrained adaptation in directional 60 ghz wlans: protocol design and system implementation," in *ACM MobiHoc 2016*, 2016.

[7] T. Wei, A. Zhou, and X. Zhang, "Facilitating robust 60 ghz network deployment by sensing ambient reflectors." in *USENIX NSDI*, 2017.

[8] M. F. Iskander and Z. Yun, "Propagation prediction models for wireless communication systems," *IEEE Transactions on microwave theory and techniques*, vol. 50, no. 3, pp. 662–673, 2002.

[9] I.-R. P.2040-1, *Effects of building materials and structures on radiowave propagation above about 100 MHz*, International Telecommunication Union Recommendation ITU-R, July 2015.

[10] J. Lu, D. Steinbach, P. Cabrol, P. Pietraski, and R. V. Pragada, "Propagation characterization of an office building in the 60 ghz band," in *IEEE EuCAP*, 2014.

[11] M.-K. Hu, "Visual pattern recognition by moment invariants," *IRE transactions on information theory*, vol. 8, no. 2, pp. 179–187, 1962.

[12] G. Durgin and T. Rappaport, "Basic relationship between multipath angular spread and narrowband fading in wireless channels," *Electronics Letters*, vol. 34, no. 25, pp. 2431–2432, 1998.

[13] O. Abari, D. Bharadia, A. Duffield, and D. Katabi, "Enabling high-quality untethered virtual reality," in *USENIX NSDI*, 2017.

[14] İ. K. Altınel, N. Aras, E. Güney, and C. Ersoy, "Binary integer programming formulation and heuristics for differentiated coverage in heterogeneous sensor networks," *Computer Networks*, vol. 52, no. 12, pp. 2419–2431, 2008.

[15] R. M. Karp, "Reducibility among combinatorial problems," in *Complexity of computer computations*. Springer, 1972, pp. 85–103.

[16] J. Ai and A. A. Abouzeid, "Coverage by directional sensors in randomly deployed wireless sensor networks," *Journal of Combinatorial Optimization*, vol. 11, no. 1, pp. 21–41, 2006.

[17] M. Communications, *WARP v3 Kit*, 2012, retrieved on 2017-06-16 from https://www.mangocomm.com/products/kits/warp-v3-kit.

[18] VubIQ, *https://www.pasternack.com/60-ghz-systems-and-modules-category.aspx*, 2015.

[19] A. Yahya, *LTE-A Cellular Networks: Multi-hop Relay for Coverage, Capacity and Performance Enhancement*. Springer, 2016.

[20] B. Langen, G. Lober, and W. Herzig, "Reflection and transmission behaviour of building materials at 60 ghz," in *IEEE PIMRC 1994*, 1994.

[21] S. K. Saha, V. V. Vira, A. Garg, and D. Koutsonikolas, "A feasibility study of 60 ghz indoor wlans," in *IEEE ICCCN 2016*, 2016.

[22] Z. Yang, P. H. Pathak, Y. Zeng, and P. Mohapatra, "Sensor-assisted codebook-based beamforming for mobility management in 60 ghz wlans," in *IEEE MASS 2015*, 2015.